SMART – A SMALL PARTICLE ACCELERATOR ON CHIP

A. Marcia *[1], E. Corte, R. H.Wilton, A. Picciotto
Fondazione Bruno Kessler (Sensor and Devices, NEXT unit), Trento, Italy
[1]also at University of Trento, Trento, Italy

Abstract

The miniaturization of particle accelerators via Dielectric Laser Acceleration (DLA)offers a route to ultra-compact, cost-effective devices powered by commercial laser systems. This work explores the extension of DLA technology—historically focused on electrons—to protons, aiming to enable "on-chip" sources of high energy hadrons. We present the design and simulation of a novel microstructure optimized for the acceleration of non-relativistic protons. Key challenges addressed include the management of phase slippage and the requirement for strong transverse confinement of heavy particles at low β. This study aims to demonstrate the potential for stable acceleration and focusing, validating the pDLA(proton-DLA) concept as a viable candidate for future compact accelerator architectures.

INTRODUCTION

Dielectric laser-driven accelerators (DLAs) [1] are currently the subject of extensive research as a cornerstone for the next generation of compact particle sources. The fundamental advantage of DLAs over conventional radio-frequency (RF) metallic accelerators lies in the superior Laser-Induced Damage Threshold (LIDT) of dielectric materials at optical and near-infrared frequencies. While traditional metallic cavities are strictly limited by surface breakdown and vacuum discharge typically constraining accelerating gradients to below 100 MV/m dielectric structures can sustain electromagnetic fields in the GV/m regime when driven by ultra-short laser pulses. This high-gradient capability allows for a radical miniaturization of the accelerating distance, potentially reducing kilometer-scale infrastructures to millimetric chip-scale devices. Leveraging these unique characteristics, recent investigations have moved beyond the ultra-relativistic electron regime to explore the application of DLA technology for proton acceleration [2]. The transition to hadrons presents significant opportunities for developing portable ion sources for nuclear physics and cost-effective, chair-side proton therapy systems. However, this extension requires sophisticated structural designs to maintain phase synchronicity in the non-relativistic regime ($\beta \ll 1$), where the grating periodicity Λ must be precisely tapered to match the evolving velocity of the heavier particles. These advancements underscore the versatility of DLAs as a transformative platform for both fundamental research and medical applications. This paper investigates the acceleration of protons in a double-grating structure [3], performing a comprehensive parameter study to maximize both fabrication feasibility and the achievable accelerating gradient. By optimizing the structural geometry and laser-matter interaction, we aim to bridge the gap between theoretical high-gradient performance and the practical constraints of modern nano-fabrication. To achieve this, numerical optimizations are performed using the CST Studio Suite [4]. The structural geometry is primarily optimized through Finite-Difference Time-Domain (FDTD) simulations to characterize the electromagnetic field distribution and maximize the synchronous accelerating components within the vacuum channel. This approach ensures that the design maintains phase synchronicity for non-relativistic particles ($\beta < 1$) while preserving beam quality and stability during the high-gradient acceleration process.

* amarcia@fbk.eu

OPTIMIZATIONS FOR ACCELERATION OF NON RELATIVISTIC PROTONS

Upon dual-sided illumination of a double-grating structure by counter-propagating laser beams, the coherent diffraction of the optical fields facilitates the excitation of multiple spatial harmonics. In the regime of non-relativistic proton acceleration, achieving efficient energy gain is strictly dependent on the synchronicity condition, formulated as $\lambda_p = n\lambda_0\beta$ where λ_p denotes the grating period (as illustrated in Fig. 1), β represents the relativistic velocity factor of the particle, and the integer n defines the harmonic order, characterizing the number of optical cycles elapsed per grating period.

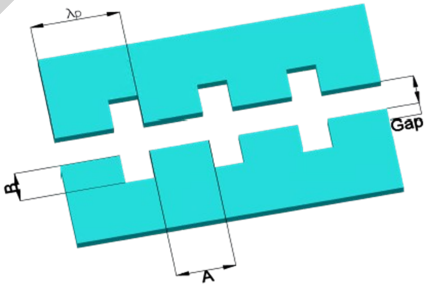

Figure 1: CAD schematic of the double-grating dielectric structure. The labels indicate the geometric dimensions required to satisfy the phase-matching conditions.

As expressed by the synchronicity condition, the non-relativistic nature of the protons imposes rigorous constraints on the geometric fabrication parameters of the dielectric structure. Numerical simulations were performed using a monochromatic plane wave with a central wavelength of $\lambda_0 = 2\,\mu$m. The structure was modeled using Fused Silica (SiO_2, refractive index $n = 1.53$), selected for its high optical transparency and superior laser-induced damage threshold

(LIDT), which are critical for sustaining high accelerating gradients.

The proton bunch is characterized by an injection kinetic energy of 100 keV [5], corresponding to a relativistic velocity factor of $\beta = 0.01459$. The selection of this specific energy regime is dictated by the requirement for compact and portable particle sources, which are essential to ensure efficient beam coupling into the sub-wavelength accelerating channels of the dielectric structure.

Such a miniaturized footprint is a key design constraint for the realization of integrated laser-driven accelerators [2]. To satisfy the phase-matching requirements at this velocity, the grating period λ_p must be precisely tailored to the specific spatial harmonic n excited within the structure. Utilizing the synchronicity condition previously described, the required grating periods for the first three spatial harmonics ($n = 1, 2, 3$) are summarized in Table 1, assuming a fixed driving wavelength of $\lambda_0 = 2\,\mu m$.

Table 1: Calculated grating periods λ_p for the first three spatial harmonics at an injection energy of 100 keV ($\beta = 0.01459$) and a driving wavelength $\lambda_0 = 2\,\mu m$.

Harmonic Order (n)	**Grating Period λ_p (µm)**
1	0.029
2	0.058
3	0.087

As evidenced by the results in Table 1, the low velocity of non-relativistic protons results in extremely small structural dimensions. These sub-100 nm features approach the fundamental resolution limits of modern lithographic techniques. Specifically, the fabrication of structures corresponding to the first harmonic ($n = 1$) represents a significant technical challenge, as the required periodicity of 29 nm pushes the boundaries of state-of-the-art electron-beam lithography and subsequent etching processes. Consequently, to mitigate fabrication complexities and ensure structural integrity, the present work focuses exclusively on the configuration corresponding to the third spatial harmonic ($n = 3$). This choice provides a more feasible grating period of 87 nm, representing an optimal trade-off between the excitation of higher-order harmonics and the practical constraints of current lithographic techniques.

SIMULATION RESULTS AND PARAMETRIC OPTIMIZATION

In order to optimize the dielectric structure (as depicted in Fig. 1), a comprehensive parametric study was performed. The optimization process involved evaluating the peak accelerating gradient as a function of the geometric variations of the structure's parameters. By systematically sweeping the critical dimensions, we identified the configuration that maximizes the longitudinal electric field while maintaining the synchronicity required for efficient proton acceleration. This sensitivity analysis is crucial for determining the fabrication tolerances necessary to preserve high-gradient performance in a practical experimental setup. Figure 2 illustrates the dependence of the accelerating gradient on the gap width.

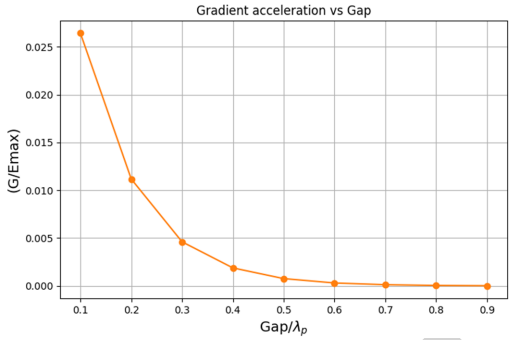

Figure 2: Simulated accelerating gradient as a function of the vacuum gap width. The data highlights the transition between the high-field evanescent regime and the reduced coupling observed at larger apertures.

As demonstrated by the simulation results, there is a clear trade-off between the field strength and the clearance for the beam; while narrower gaps enhance the coupling of the longitudinal electric field, they also impose stricter requirements on beam emittance and alignment.

The structural parameters A (pillar width) and B (pillar height) were systematically optimized to maximize the accelerating gradient. Figure 3 illustrates the dependence of the gradient on the normalized width A/λ_p. The observed pattern is characterized by a non-monotonic, oscillatory behavior, which is indicative of complex interference effects and spatial harmonic coupling within the dielectric gap. The peaks at $A/\lambda_p \approx 0.2, 0.5$, and 0.9 represent resonant conditions where the field enhancement is maximized, while the dip at 0.7 suggests a destructive interference regime that should be avoided during fabrication.

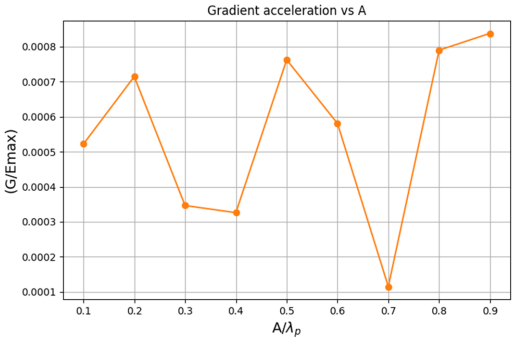

Figure 3: Normalized accelerating gradient (G/E_{max}) as a function of the pillar width A/λ_p normalized to the grating period λ_p.

In contrast, the impact of the height of the pillar B is shown in Fig. 4. In this case, the accelerating field exhibits a sharp initial increase followed by a clear asymptotic saturation for $B/\lambda_p > 0.3$.

This plateau indicates that once the pillars exceed the minimum height required for effective scattering, further increases in B do not significantly enhance the acceleration performance. This result is particularly favourable for nano

fabrication, as it implies a high degree of robustness against vertical etching tolerances, provided the minimum threshold is met.

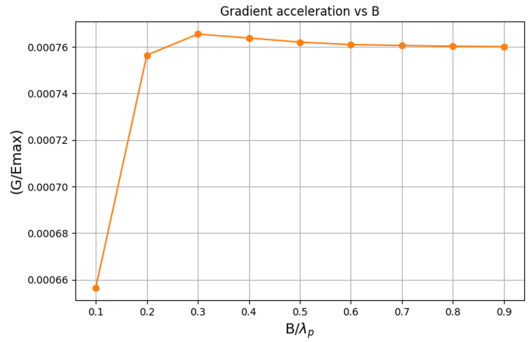

Figure 4: Normalized accelerating gradient ($G/E_{\max}$) as a function of the normalized pillar height B/λ_p, showing a characteristic saturation plateau.

Following the parametric optimization of the double-grating geometry, a set of final design parameters was selected to maximize the accelerating gradient while ensuring feasible nanofabrication for 100 keV protons.

The optimized dimensions are summarized in Table 2. The gap width was fixed at 35 nm to provide an optimal balance between field enhancement and beam clearance. For the pillar geometry, both the width and height were set to 44 nm. This corresponds to a normalized width of $A/\lambda_p \approx 0.5$, which aligns with the primary resonance peak observed in Fig. 3, and a normalized height of $B/\lambda_p \approx 0.5$, ensuring the structure operates well within the saturation plateau shown in Fig. 4.

Table 2: Optimized geometric parameters for the dielectric laser accelerator structure ($n = 3$, $\lambda_0 = 2\,\mu$m, $\beta = 0.01459$).

Parameter	Dimension (µm)
Grating period (λ_p)	0.087
Vacuum gap	0.035
Pillar width (A)	0.044
Pillar height (B)	0.044

With the structural parameters finalized, the longitudinal electric field (E_{acc}) was characterized along a single grating period λ_p. This analysis is critical to verify the effective accelerating gradient experienced by the synchronous proton bunch at the optimal injection phase.

Figure 5 displays the local accelerating field distribution. The field exhibits a clear periodic modulation, consistent with the excitation of the third spatial harmonic ($n = 3$). The peak local fields reach magnitudes exceeding 4 GV/m; however, the effective accelerating gradient (G), calculated by averaging the field over the transit period, is determined to be $G_{\text{opt}} = 34.31$ MV/m (as indicated by the dashed reference line). This result confirms that the optimized dielectric structure can sustain significant accelerating gradients even in the non-relativistic regime, providing a robust baseline for further beam dynamics studies.

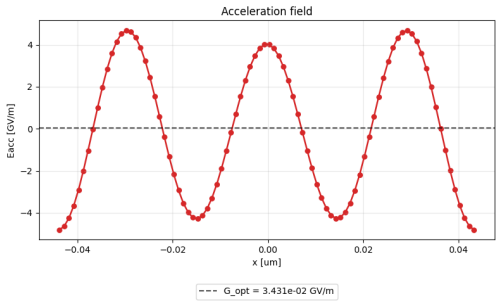

Figure 5: Local accelerating field E_{acc} as a function of the longitudinal position x over one grating period. The dashed line represents the effective average gradient $G_{\text{opt}} = 34.31$ MV/m at the optimal phase.

CONCLUSION

We numerically optimized a silica-based double-grating structure for accelerating 100 keV protons and showed that operating on the third spatial harmonic ($n = 3$) can yield an effective accelerating gradient of 34.31 MV/m.

Our parametric analysis indicates that the required sub-100 nm periods and features down to 35 nm lie at the edge of current nanofabrication capabilities, imposing stringent electron-beam lithography and etching tolerances and limiting scalability and experimental reliability. A promising approach to relax these constraints is to increase the driving laser wavelength (λ_0). Because the synchronicity condition scales the grating period λ_p linearly with λ_0, moving to the mid-infrared would allow larger feature sizes. This shift, however, requires exploring alternative dielectrics, as fused silica (SiO_2) becomes absorbing at longer wavelengths.

Future work will therefore focus on integrating wide-bandgap, infrared-transparent materials to enable a new generation of DLAs that combine high performance with improved practicality and experimental robustness.

REFERENCES

[1] E. A. Peralta *et al.*, "Demonstration of electron acceleration in a laser-driven dielectric microstructure", in *Nature*, vol. 503, no. 7474, pp. 91-94, Nov. 2013. doi:10.1038/nature12664

[2] G. Torrisi *et al.*, "Feasibility study and perspectives of proton Dielectric Laser Accelerators (p-DLA): from nanosource to accelerator scheme", *arXiv*, Jun. 2021. doi:10.48550/arXiv.2106.13701

[3] T. Plettner *et al.*, "Proposed few-optical cycle laser-driven particle accelerator structure", *Phys. Rev. ST Accel. Beams*, vol. 9, no. 11, p. 111301, Nov. 2006. doi:10.1103/PhysRevSTAB.9.111301

[4] CST Studio Suite, SIMULIA - Dassault Systèmes. https://www.3ds.com/simulia.

[5] A. Marcia, R. Hall-Wilton, and A. Picciotto, "Design and optimization of an on-chip electrostatic injector for a miniaturized proton/ion linear accelerator", *EPL*, vol. 154, no. 54001, Apr. 2026. doi:10.1209/0295-5075/AE6729